Reviews in Mineralogy & Geochemistry
Vol. 80 pp. 165-190, 2015

Precipitation in Pores: A Geochemical Frontier

Andrew G. Stack

Chemical Sciences Division
Oak Ridge National Laboratory
Oak Ridge, Tennessee 37831-6110, USA

stackag@ornl.gov

INTRODUCTION

The purpose of this article is to review some of the recent research in which geochemists have examined precipitation of solid phases in porous media, particularly in pores a few nanometers in diameter (nanopores). While this is a "review," it is actually more forward-looking in that the list of things about this phenomenon that we do not know or cannot control at this time is likely longer than what we do know and can control. For example, there are three directly contradictory theories on how to predict how precipitation proceeds in a medium of varying pore size, as will be discussed below. The confusion on this subject likely stems from the complexity of the phenomenon itself: One can easily clog a porous medium by inducing a rapid, homogeneous precipitation directly from solution, or have limited precipitation occur that does not affect permeability or even porosity substantially. It is more difficult to engineer mineral precipitation in order to obtain a specific outcome, such as filling all available pore space over a targeted area for the purposes of contaminant sequestration. However, breakthrough discoveries could occur in the next five to ten years that enhance our ability to predict robustly and finely control precipitation in porous media by understanding how porosity and permeability evolve in response to system perturbations. These discoveries will likely stem (at least in part) from advances in our ability to 1) perform and interpret X-ray/neutron scattering experiments that reveal the extent of precipitation and its locales within porous media (Anovitz and Cole 2015, this volume), and 2) utilize increasingly powerful simulations to test concepts and models about the evolution of porosity and permeability as precipitation occurs (Steefel et al. 2015, this volume). A further important technique to isolate specific phenomena and understand reactivity is also microfluidics cell experiments that allow specific control of flow paths and fluid velocities (Yoon et al. 2012). An improved ability to synthesize idealized porous media will allow for tailored control of pore distributions, mineralogy and will allow more reproducible results. This in turn may allow us to isolate specific processes without the competing and obfuscatory effects that hinder generalization of observations when working with solely natural samples. It is likely that no one single experiment, or simulation technique will provide the key discoveries: to make substantive progress will require a collaborative effort to understand the interplay between fluid transport and geochemistry. Where rock fracturing and elevated pressures are of concern, an understanding and capability to model geomechanical properties are necessary (Scherer 1999).

It is critical to understand not just how the precipitation reactions themselves occur, but how a given solution composition, net flow rate and porous substrate translate to macroscopic hydrologic parameters such as the evolution porosity and permeability that change in response to geochemical reactions. Predicting these macroscopic terms is prerequisite for extrapolating from laboratory-based or *in silico* (i.e., computational model) systems where every pore in

1529-6466/15/0080-0005$05.00 http://dx.doi.org/10.2138/rmg.2015.80.05

the reactor/cell can be resolved or sampled to reservoir-scale simulations and field studies. In these larger length-scale studies, it is no longer practical to think about individual pores but instead one must consider pore distributions in aggregate. The current state-of-the-art is to use linear relationships where the porosity and permeability are calculated using empirically fit functions (Gibson-Poole et al. 2008). To improve the status quo will require us to develop new, up-scaling theories that can accurately approximate the richness of reactivity observed at the atomic- to pore-scales, but are still useful at the reservoir scale (Reeves and Rothman 2012). To verify and validate such models will require a strong connection between research performed at the nanometer- or micrometer-length scales and larger column- or field-scale studies.

RATIONALE

A capability to predict and control precipitation in pores could result in more useful geochemistry in many situations in the subsurface, and in this section a few of them will be described. A good first example of where precipitation is important is the well known two order of magnitude discrepancy between field-based and laboratory-based rates of mineral weathering reactions (Drever and Clow 1995; White 2008; Stack and Kent 2015). There are abundant theories for the origin of the discrepancy, but two particularly important for this article are the existence of pore-size-dependent effects (Putnis and Mauthe 2001; Emmanuel and Ague 2009; Stack et al. 2014) and secondary mineral formation that reduces the reactive surface area (Drever and Clow 1995; Maher et al. 2009). Maher et al. (2009) in particular showed in a chronosequence of soils that laboratory-based dissolution rates can be consistent when precipitation of secondary phases is accounted for. The effect of secondary mineral precipitation on weathering will become even more significant if the extent of precipitation is large enough such that the permeability of the soil or rock is significantly degraded and flow of fluids through the rock is impeded. Mineral weathering itself is important for understanding the composition of ground and surface waters, and minerals act as the longer term buffer of carbon dioxide in the atmosphere (Berner et al. 1983) and acidity in rain (Drever and Clow 1995).

In addition to natural processes, engineered precipitation in porous media is being explored as a contaminant sequestration and remediation strategy. It may be possible to take advantage of the low solubility of some minerals to remediate metal contaminants intentionally. An example includes radium, which readily substitutes for barium in barite ($BaSO_4$) due to similar reaction behavior and size of radium and barium. Radium is an issue for spent nuclear fuel repositories that use bentonite as a sorbent since radium does not adsorb strongly to clay minerals (Curti et al. 2010). However, there is evidence that the mobility of radium is effectively controlled by barite solubility (Martin et al. 2003) because so much radium can incorporate into barite and barium is more common than radium. Already a method that takes advantage of the low solubility of Ba–Ra–Sr sulfate minerals has been proposed as an above-ground treatment strategy for hydraulic fracturing wastewater (Zhang et al. 2014), but it may be possible to utilize this for subsurface applications in porous media. Another example is that of uranium, which potentially could be remediated using hydroxyapatite which dissolves and causes a uranium phosphate precipitate to form (Arey et al. 1999; Fanizza et al. 2013). Instead of using abiotic hydroxapatite directly, less expensive bone meal has been considered (Naftz et al. 1998). When used as a permeable reactive barrier, the extent of this precipitation is such that the bone meal needs to be diluted with unreactive phases to avoid clogging the reactive barrier by reducing the permeability drastically (Naftz et al. 1998). To avoid the issue of clogging, other studies have examined the idea of using a soluble organo-phosphate that is degraded by bacteria in the subsurface to create dissolved inorganic phosphate, which can

then react with the uranium (Wright et al. 2011; Beazley et al. 2007). This concept is attractive since an aqueous solution containing the organo-phosphate could be injected into a well, where it would presumably mix with ambient fluids and become dispersed. The microbially induced cleavage of the organophosphate would cause the dissolved inorganic phosphate concentration to increase over time and lead to precipitation of uranium phosphate. A final example metal contaminant is strontium-90, which is found sometimes as a legacy waste from nuclear weapons production (Riley et al. 1992). Due to the similar chemical behavior and size of strontium and calcium, strontium incorporates into the calcite ($CaCO_3$) crystal lattice (Wasylenki et al. 2005; Bracco et al. 2012). If one could therefore induce precipitation of a strontium-rich calcite, the contaminant would be trapped as a solid phase and immobilized. Immobilization for approximately one hundred years would be sufficient time to allow the strontium-90 to decay to stable zirconium (Gebrehiwet et al. 2012), which in turn is incredibly insoluble (Wesolowski et al. 2004). It is not unreasonable to think that a calcite precipitate formed in the subsurface could last that long. As one of the authors in the Gebrehiwet et al. (2012) study suggested, however, one can only control three things in regards to induced precipitation in the subsurface: what solution one injects, where one injects it and how fast one does so (Redden G.; pers. commun.). Thus for a remediation scheme of this type to work in the subsurface, as opposed to in a soil or engineered reactive barrier, one would need to have a precise control over where precipitation takes place, how fast precipitation occurs and an understanding of how that precipitate changes the pore structure and communication of the fluid. This level of control of precipitation has not been demonstrated to my knowledge, but perhaps is not as far-fetched as one might initially guess. The issues involve being able to balance mixing of an injected fluid with the ambient groundwater and/or other injected fluids containing reactants, and the timing of precipitation reactions within the porous medium. However, as discussed above, permeability should be maintained while the precipitation reaction is ongoing if possible, i.e., until all of the contaminant is successfully sequestered in a solid phase. The precipitation should therefore not occur too quickly, otherwise the calcite will form too close to the injection well and clog, nor too slowly so that the strontium and injected fluids disperse prior to precipitation occurring. This might be described as a "Goldilocks" problem in mineral precipitation kinetics, get it to occur not too quickly, nor too slowly, but just right.

By far the most common contaminant by mass that has been proposed to be sequestered by induced precipitation is carbon dioxide. There has been and continues to be intense research and pilot projects whose goal is to determine the feasibility of widespread sequestration of this contaminant. Despite the effort, there is still uncertainty about how much carbonate-containing mineral will precipitate (if any), the locales in which it will precipitate and how long the reactions will take. The conventional wisdom is that it will take something on the order of 1000 years to convert the carbon dioxide to a mineral (Metz et al. 2005). That is likely true in some situations, e.g., a storage reservoir that is a clean quartz sand and contains few highly reactive minerals such as the Sleipner field in the North Sea. However there are also some real world examples where significant mineral precipitation has either been directly observed, or evidence has been discovered that it may be occurring. In Nagaoka, Japan, some pore fluids have become supersaturated with respect to calcite only a few years after injection of CO_2 started (Mito et al. 2008). In a site in west Texas where CO_2 was injected over a period of 35 years for the purpose of enhanced oil recovery, fractures sealed with calcite can be observed in well casing cement (Carey et al. 2013). The latter example raises a particularly interesting possibility, which is that even if the net amount of carbon dioxide turned to a mineral is small, there could be enough precipitation to affect the storage security of a site. In this case, fractures in the well casing cement were sealed with calcite. One might expect that something similar could happen in a cap rock or seal that has had fractures open or form in it due to the increased pressure from the carbon dioxide injection. In what might be a maximum amount of precipitation observed

thus far (for the available porosity) has been during CO_2 injection in the Columbia River basalts. It appears that mineral precipitation begins immediately after injection, to the extent that pumps can get clogged and shut down (Fountain 2015). Substantial calcite precipitation is also suspected during CO_2 injection tests in basalt in Iceland. One caution is that in the basalt injection tests have all been relatively small amounts of CO_2 (kilotons), far short of the amount that would be needed to be sequestered to have an impact on the climate which are megatons to gigatons. In all three of the cases listed here where precipitation has been observed (or could occur), there has been substantial amounts of reactive mineral phases that buffer the pH and/or supply the cations necessary to cause carbonate minerals to precipitate. While some modeling studies have been undertaken to examine how much carbonate mineral can be precipitated for a given mineralogical composition (Zhang et al. 2013), what is lacking are direct measurements of how porosity and permeability evolve in a rock during the dissolution of pH-buffer and cation-source minerals and precipitation of carbonates. If precipitation occurs completely uniformly, it could be that residual bubbles of CO_2 in the subsurface left over from plume migration would become surrounded by a self-limiting coating of carbonate mineral that prevents further reaction of the gas within the bubble (Cohen and Rothman 2015) (Fig. 1). This may not be a detrimental outcome since the precipitated material might also act as a protective casing surrounding the CO_2 that prevents its migration, but it would slow and limit carbonate mineral precipitation.

An important ongoing issue in industrial or municipal settings is the prevention and removal of scale, i.e., unintended mineral precipitates that form in the (porous) subsurface as well as within wells, pipes and equipment. Entire textbooks have been written on the subject of attempting to predict the formation of the most common scale-forming minerals and dealing with them after their formation (e.g., sparingly soluble salts such as barite, $BaSO_4$, calcite, $CaCO_3$, as well as covalently bonded phases such as silica or quartz, SiO_2 and iron oxides, Fe_2O_3) (Frenier and Ziauddin 2008). It has been estimated that scale formation results in 1.4 billion USD costs annually due to lost production and removal (Frenier and Ziauddin 2008). New extraction technologies such as the combination of hydraulic fracturing and horizontal drilling are resulting in new scale formation and removal challenges as well as treatment of wastewater. An improved ability to predict and control precipitation reactions in porous media, i.e., prior to the fluids coming to the surface, could help to deal with these issues. If we could better predict and control reactions within porous media especially, it could help us understand

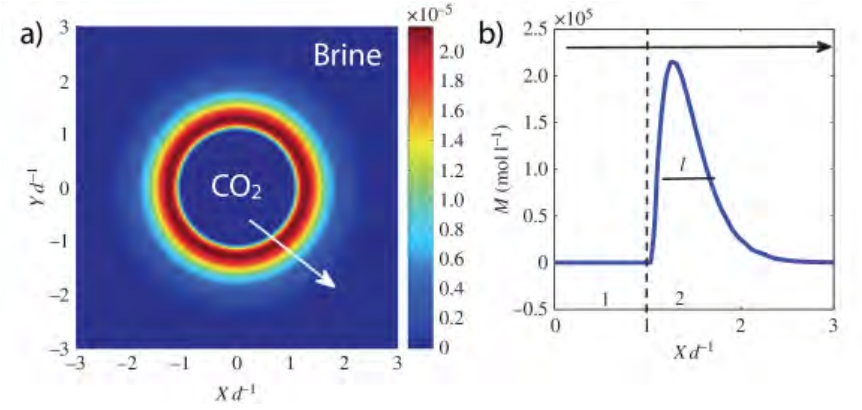

Figure 1. Model of mineral precipitation due to mixing of CO_2-rich fluids with surrounding brine. a) The warmer (lighter gray) colors show where precipated carbonate minerals are predicted to occur, creating a zone of low permeability between the two liquids and self-limiting the precipitation reaction. Units on *X* and *Y* are characteristic lengths. b) Profile along the white arrow marked in part a). [Images slightly modified from Cohen and Rothman (2014), *Proceedings of the Royal Society of London A,* Vol. 471, 2010853. Creative Commons license, v.4.0]

why scale does or does not form in a given scenario, and may guide us to treatment strategies, either above ground or directly in the subsurface prior to extraction. As a specific example, some of the wells in the Marcellus shale are producing elevated concentrations of radium, strontium and barium in their flowback or formation waters. All of these cations form low solubility sulfate minerals that clog porosity, wells, lines and equipment and have been found in effluents of wastewater treatment plants that accepted hydraulic fracturing wastewater and in sediments downstream (Ferrar et al. 2013; Warner et al. 2013). The economic and environmental ramifications of these dissolved species and their mineral forms have been significant. These findings were part of the rationale for the U.S. state of Pennsylvania's request that municipal wastewater treatment plants stop accepting hydraulic fracturing wastewater (Boerner 2013). The uncertainties surrounding the public health effects of radium-containing scale were also cited in the U.S. State of New York Department of Health review that led to the state banning hydraulic fracturing completely (Zucker 2014). It is clear that we would benefit from an improved ability to predict why ambient fluids in the subsurface do not have precipitated minerals in them, and why precipitation only occurs after the fluids are brought up to the surface. Furthermore, if precipitation of scale forming minerals could be engineered *in situ*, without impacting the oil or gas production, it would prevent costly treatment strategies and obviate environmental impact of the oil and gas production.

A sometimes overlooked set of effects of precipitation in pores are geomechanical. That is, when rocks, cements or other porous materials have fluids circulate through them that induce crystallization, the precipitated material exerts a pressure on the rock itself and vice versa. Over time, this pressure can be sufficiently large to crack or fracture a rock (Scherer 1999; Emmanuel and Ague 2009). The physics of this process are discussed in Emmanuel et al. (2015, this volume). This phenomonon has dramatic implications for weathering of rocks as it is a coupled chemical and physical process and the resulting fractures will act as conduits for new fluid that will further increase weathering rate (Jamtveit et al. 2011). Geology undergraduates can likely tell you the mechanisms of an every-day example of this process, which is pothole formation in asphalt concrete during frost wedging or heaving. When water freezes, its crystal structure is slightly less dense than the original water, and this causes exerts a force on the sand grains, wedging them apart. The crystallization pressure due to precipitation in pores may also play a role on a much larger scale than potholes or even weathering: it was recently suggested that precipitation of anhydrite ($CaSO_4$) in pores may result in micro-seismicity near mid ocean ridges (Pontbriand and Sohn 2014). The evidence is that the seismic signature and locale of the earthquakes does not match those of a tectonic origin and are not correlated with any larger seismicity in the area. The proposed mechanism is that there is secondary circulation of seawater near the ridge, which causes anhydrite to precipitate as the seawater heats. This is because anhydrite has a retrograde solubility, meaning it becomes less soluble with increasing temperature. Upon seeing this argument, one is tempted to speculate about whether precipitation could be a contributing factor in other seismic events, such as during injection of wastewater (e.g., the Youngstown, Ohio earthquake was attributed to injection of hydraulic fracturing fluids; Funk 2014; Skoumal et al. 2015). This possibility has been raised for carbon sequestration as well (Melcer and Gerrish 1996), but there is no information at all on the potential for precipitation reactions to induce seismicity.

In all the above examples, our understanding of precipitation in pores is poor in that we can define what we would like to have happen, but have trouble demonstrating that it is happening or can happen outside of some obvious indicator like the pump clogging or exhuming a reacted rock core to look for mineral precipitates. This leads to an inability to predict reliably the extent, timing and locale (e.g., pore-size distribution) of precipitation in reactions. In the remainder of this review, I summarize what I know about how precipitation in a porous medium will occur. While everything described in this article is reasonably plausible, some evidence and theories

are contradictory and sorting through which effects are important at a given time and length scale will require the substantial interdisciplinary effort described in the introduction.

PORE-SIZE-DEPENDENT PRECIPITATION

When reviewing the studies that have considered a pore size dependence for precipitation reactions, one can find a plausible argument in the literature for any trend in the dependence on pore size, or a lack thereof. That is, one can find models for uniform precipitation over all pore sizes with no intrinsic pore-size dependence (Borgia et al. 2012) (Fig. 2b), observations that precipitation in smaller pores is inhibited (Emmanuel et al. 2010) (Fig. 2c), theoretical predictions that precipitation should occur preferentially in smaller pores (Hedges and Whitelam 2012) (Fig. 2d) and observations of different behaviors depending on system chemistry (Stack et al. 2014). This lack of consensus arises from several factors, not the least of which is that this discrepancy may be real and the functional form of any pore-size-dependent behavior that is observed depends on the substrate and precipitate compositions and structures, or solution conditions. At this time we do not know precisely which processes are most important to determine the pore size range over which precipitation occurs, and further information is necessary to make reliable predictions. The length scale over which the precipitation is observed may be important as well—processes that occur at one length scale or mineral growth regime may not be significant in all cases. For example, processes important during the incipient stages of nucleation may not be important after aggregation and growth of the nuclei into larger crystals.

Effects of precipitation on porosity and permeability

Prior to getting into the details, it is useful to discuss the reasons why a pore-size dependent precipitation should matter, especially for larger scale properties. As mentioned above, one

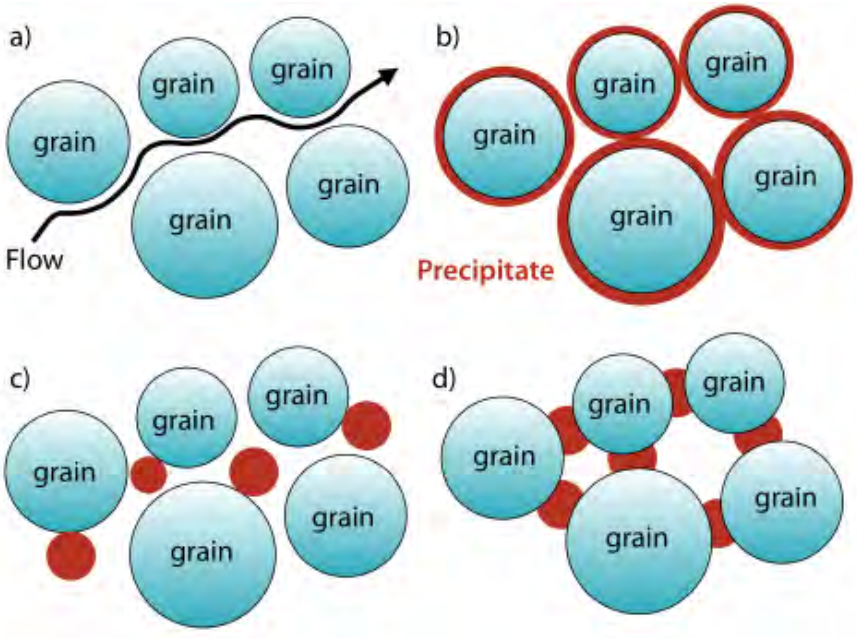

Figure 2. Schematic of pore-size dependence for precipitation reactions. a) Illustrative flow path through a series of mineral grains within a rock. b) Rock after precipitation that uniformly coats all grains. The pore throats close first, reducing permeability, but the larger pores are left mostly open. c) Preferential precipitation in large pores. d) Preferential precipitation in smaller pores. Pore throats will close first, strongly reducing permeability while having a minimal impact on porosity.

area where advanced understanding is necessary is the link between porosity and permeability. If significant precipitation in a porous medium occurs, the effect of the precipitation on the porosity and permeability cannot be neglected. While one can estimate change in porosity based on the amount of precipitated material and its molar volume, the effect of that porosity change has on the permeability and the ultimate extent of reaction will vary depending on how the precipitation affects the flowpaths that dominate the transport of fluids through the medium. This in turn could potentially affect how the much material can be precipitated prior to the reaction becoming limited by the transport of new reactants to the site of precipitation. An example of this behavior is the CO_2 bubble study above (Cohen and Rothman 2015), where the model indicated that the precipitation reaction was self-limiting because the change in permeability stopped the subsequent dissolution of CO_2 gas into the aqueous phase (Fig. 1). This is despite the fact that the overall system is still very far from equilibrium.

The textbook method to estimate permeability is to express it as proportional to the square of the grain size, such as observed using glass beads (e.g., Freeze and Cherry 1979):

$$k = Cd^2, \tag{1}$$

where the permeability, k, has units of length squared, C is a fit parameter, and d is the average grain diameter. (The common units of permeability are in Darcy, where 1 Darcy $\cong 10^{-8}$ cm^2). The larger the grain, the larger the pore size, and much larger is the permeability. While this simple expression is interesting to think about, in practice is only useful if mineralogy and other parameters such as grain shape remain more or less constant across samples. For example, an analysis of Gibson-Poole et al. (2008) find over three orders of magnitude variation in permeability for a given porosity for samples from a single formation across a potential CO_2 storage basin (Fig. 3). Moreover, precipitation reactions may have non-linear effects on permeability: Tartakovsky et al. (2008) found that an impermeable layer of $CaCO_3$ could form within a reactor with only a 5% reduction in porosity (see below). From these studies it is clear that porosity alone cannot be used to predict permeability, therefore one can incorporate additional empirical parameters that affect permeability, such as (Bloch 1991; Zhang et al. 2013):

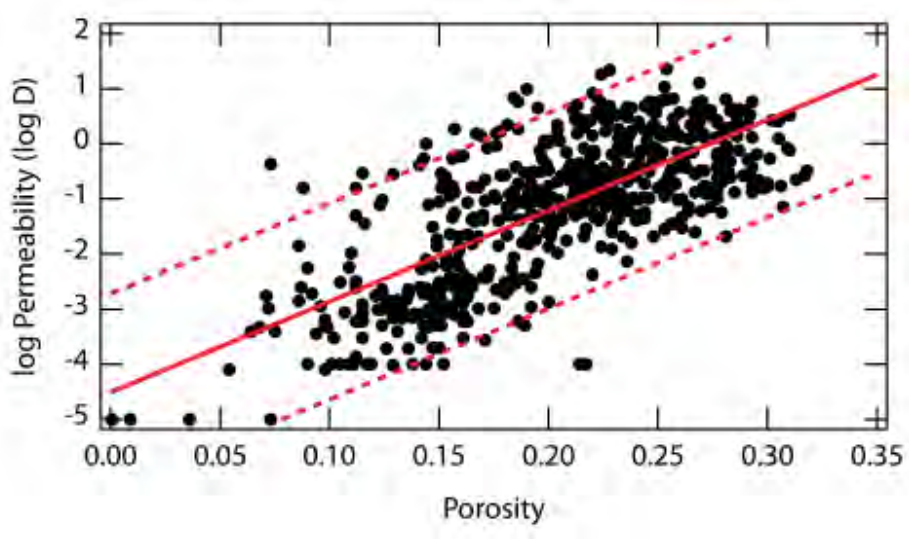

Figure 3. Log permeability as a function of porosity in two different formations across a potential CO_2 sequestration reservoir. Data from Gibson-Poole et al. (2008) for a single rock formation. Trendline is a best fit for log permeability as a function of porosity, dashed lines are the 95% prediction interval. The prediction intervals span more than three orders of magnitude in permeability.

$$\log_{10} k = d + e \times \text{grain size} + \frac{e}{\text{sorting}} + f \times \text{rigid grain content}, \quad (2)$$

where *a–f* are fit parameters. Here, the dependence of permeability on grain size is exponential, consistent with observations (Freeze and Cherry 1979; Gibson-Poole et al. 2008).

Extrapolating Equations (1) and (2) to a distribution of pore sizes and assuming that the super-linear dependence of permeability on grain size (and hence pore size) is still valid, we can hypothesize a trend about the potential effects of a pore-size-dependent precipitation. If precipitation were to occur preferentially in the largest pores, it would have disproportionate effects on the permeability, since the largest pores are created by the largest grains and the largest grains will have the largest effect on the overall permeability (Fig. 2c). Contrarily, if precipitation occurs preferentially in the smallest pores, it might have minimal effects on the permeability since overall permeability might be, but this process may occlude pore throats, that is, the distance of closest approach between two mineral grains (Fig. 2d). This would strongly affect permeability. One behavior might be desirable over another in different situations. For example, in a cap-rock intended to restrain a plume of trapped CO_2, if precipitation occurs in the largest pores or in fractures larger than the average pore size, a minimal amount of precipitation would be responsible for a self-sealing behavior and a more efficient cap rock. Alternately, if one wanted to precipitate as much material as possible within the available pore space, such as in the reservoir rock for carbon or other contaminant sequestration, one would prefer it if permeability of the rock was maintained until the reaction is completed to avoid a self-limiting behavior. This would allow continued reactant transport to the site of reaction and mixing of various reactants. Thus one would prefer it if precipitation occurred preferentially in the smallest pores and proceed to the larger ones.

There does not necessarily need to be a pore-size-dependent precipitation to have an effect on the permeability of the medium prior to filling all the pore space. Precipitation reactions in reactive transport simulations have been modeled as uniformly coating the grains in the porous medium. As the precipitation proceeds, the pore throats become filled with precipitate but this leaves the largest pore spaces open (Fig. 2b). When this happens, permeability of the formation can also become reduced because communication and transport of fluids between pores is no longer possible. This behavior is conceptualized using the "Tubes in Series" theory (Verma and Pruess 1988), where the flow through the rock is approximated as a bundle of capillaries whose diameter is reduced in some portions, restricting the fluid flow. This technique has been used to model precipitation of evaporite minerals due to drying of the ambient fluids in a reservoir rock after CO_2 is injected. The minerals, principally halite (NaCl), substantially clog permeability of the formation (Borgia et al. 2012).

Observations of precipitation in pores

While the concept of examining the growth of minerals or other crystals from bulk solution or natural specimens has been around for a long time (see e.g., Stack 2014 for a review of calcium carbonate rates), examining how crystals grow in the middle of a porous medium has been a more difficult proposition to study because, by their nature, it is difficult to discern what is happening in the interior of rocks without irrevocably modifying and/or destroying the integrity of the sample. So until recently, most experiments and analysis of precipitation in pores have been done *ex situ*. See Putnis and Mauthe (2001) for excellent examples of mercury porosimetry analysis of dissolution experiments on precipitated material. Historically, *in situ* information has been obtained by analyzing the compositions of pore fluids (Morse et al. 1985). Sampling a pore fluid is often the only practical method to get information about the processes in the subsurface. As demonstrated in Steefel et al. (2014), the difficulty with this method is that it is inherently inferential. That is, one must infer which

minerals are precipitating and where based on their solubilities or perhaps examining how permeability might change with reduction in solution flow rate or increase in pressure. The above-mentioned advances in synthesizing samples, measuring reactivity *in situ* and modeling the outcome have the potential to allow us to observe precipitation directly over the course of an experiment and to link precipitation rates, growth regime and flow rates with porosity and permeability evolution within a sample. It remains to be seen if these advances will lead to an ability to obtain a fine-grained control over precipitation reactions in porous media and contribute to the resolution of the discrepancy between laboratory- and field-based weathering rates.

A further source of difficulty in measuring precipitation in pores is that many observations only cover a limited range of pore sizes, e.g., on thin sections or hand samples, and do not detect the smallest pore sizes. Pores size varies many orders of magnitude and the smallest pore are the interlayer spacings in clays (or their equivalent), which are on the nanometer scale. For example, a smectite clay has a *d*-spacing (or repeat distance) of 1–2 nm depending on how much water is in the interlayer (Bleam 2011). These smallest pores, termed nanopores, may dominate the overall porosity in a rock (Anovitz et al. 2013). Part of the difficulty is the limited range of pore sizes that can be analyzed using the standard tools for analyzing pore-size distributions: gas adsorption and mercury porosimetry. Gas adsorption relies on measurements of a powdered form of the rock sample, destroying the original rock fabric and may introduce a dependence of the pore size measurement on the particle size of the powder used in the experiment (Chen et al. 2015). To reach the smallest pore sizes, interpretation of mercury porosimetry relies on an assumption that the technique does not modify the sample in any way, yet to measure, e.g., a 3.5 nm pore size with this technique requires 400 MPa pressure applied to the sample (Giesche 2006). This is equivalent of burying the rock at 17 km depth using a lithostatic pressure gradient of 23 MPa/km (Bethke 1986). It is clear that compaction of the sample is a real danger in this type of measurement and restricts its typical use to larger pore sizes. Other methods to observe precipitation in pores have included optical microscopy, SEM, and microprobe analysis, but these tools also have a resolution limit of sub-micron or so at best, depending on the instrument and sample.

Previous work on pore-size-dependent precipitation also focused on monitoring the supersaturation necessary prior to nucleate materials in idealized porous media such as silica aerogel (Prieto et al. 1990; Putnis et al. 1995). What they found is there exists a threshold supersaturation that is necessary to achieve prior to the nucleation of materials becoming favorable. This was attributed to a pore-size-dependent solubility (see below), stirring rate, interaction between substrate and precipitate. Classical nucleation theory calls for a critical supersaturation necessary prior to nucleation becoming energetically favorable, but this concept is a distinct modification of the surface energy (Fig. 4) (De Yoreo and Vekilov 2003; experimental evidence of this observed in Godinho and Stack 2015). This concept is supported by some *ex situ* work on sandstone thin sections that has shown naturally formed halite cements have a tendency to occlude larger pores and are not found in smaller ones (Putnis and Mauthe 2001).

A recent Small Angle X-ray Scattering (SAXS) study on a nanoporous amorphous silica showed that nucleation in nanopores may or may not be inhibited, but depends on the surface chemistry between precipitate and substrate (Stack et al. 2014). In this work, we took the approach of measuring precipitation in both native 8-nm nanoporous amorphous silica (Controlled Pore Glass-75, or CPG-75), and CPG modified with a self-assembled monolayer containing an anhydride group, which presumably hydrolyzes in water to form a dicarboxylic acid. The idea was to have the same pore size distribution, but different surface functional groups and different surface reactivity at the substrate-water interface. Aqueous solution supersaturated with respect to calcite ($CaCO_3$) was circulated past the CPG, and the small angle X-ray

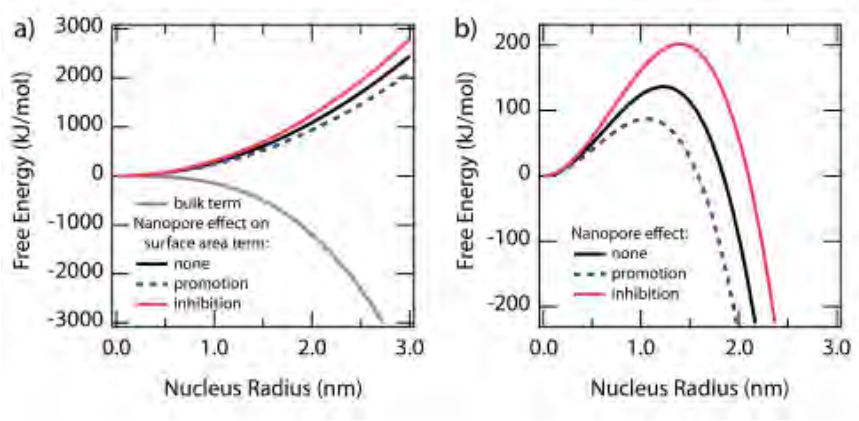

Figure 4. Classical nucleation theory, and potential effects of nanopores. a) For a growing nucleus, there are two energetic terms that determine its stability, a negative term from the bulk phase that grows with the cube of the radius and a positive surface area term that grows with the square of the radius. A nucleus growing in a nanopore will have its surface energy changed by the presence of the nanopore. b) The sum of the two terms in a), which determine the overall stability of the nucleus. The critical radius is determined by the position of the peak. If the presence of a pore increases the surface energy of the nucleus by increasing its interfacial energy, it will create a larger critical radius than in open solution. If a pore lowers the total surface energy, it will facilitate precipitation by creating a smaller critical radius, or alternately a lower supersaturation necessary for growth.

scattering was measured as the reaction proceeded. We found that where native CPG showed precipitation only in the spaces in between CPG grains (i.e., macropores ≥ 1 μm diameter), functionalizing the CPG with a polar self-assembled monolayer caused precipitation to occur in both nanopores and macropores (Fig. 5). At the time of publication, the results of this study were thought to suggest that the pore size in which the precipitation preferentially occurred was controlled by the favorability of nucleating the precipitating phase onto the substrate. While this is still a possibility, an alternate, solution-side explanation that relies on surface charge of the substrate is given below that is only briefly touched on in the previous work.

Recent work has shown that small and ultra-small angle neutron and X-ray scattering can be combined with, e.g., traditional SEM-BSE analysis to obtain a measurement of pore sizes that range seven orders of magnitude (Wang et al. 2013). This series of techniques removes one of the issues with the pore size characterization techniques described above in that the sample is not ground to a powder. The X-ray and neutron sampling are non-invasive with respect to the integrity of the sample, although working on thicker samples (e.g., 1 mm thick) tends to create multiple scattering events that are more difficult to interpret. Thus far, these techniques have primarily been used to characterize rock samples *ex situ*. Each set of techniques, Small Angle X-ray/Neutron Scattering (SAXS, SANS), Ultra SAXS/SANS, and SEM-BSE each probe only a couple orders of magnitude of pore size, but overlapping ranges allows one to join the pore size distributions derived from each technique into one master porosity distribution. Because of this requirement, however, it may be difficult to obtain reasonable results *in situ*. Lastly, there are issues with interpreting the data from these methods, such as improper background subtraction can lead to anomalous changes in the apparent porosity distribution, etc.

What has been observed thus far on rock samples the SANS/USANS/BSE-SEM techniques has been mixed. Wang et al. (2013) detected a reduced (relative) contribution to the total porosity from small scale pores in metamorphic rocks that underwent higher degrees of metamorphism. This implies that smaller pores tended to close first during the combustion and other metamorphic processes the rocks underwent over time. Alternately, Anovitz et al. (2015) found that despite being exposed to a solution supersaturated with respect to quartz

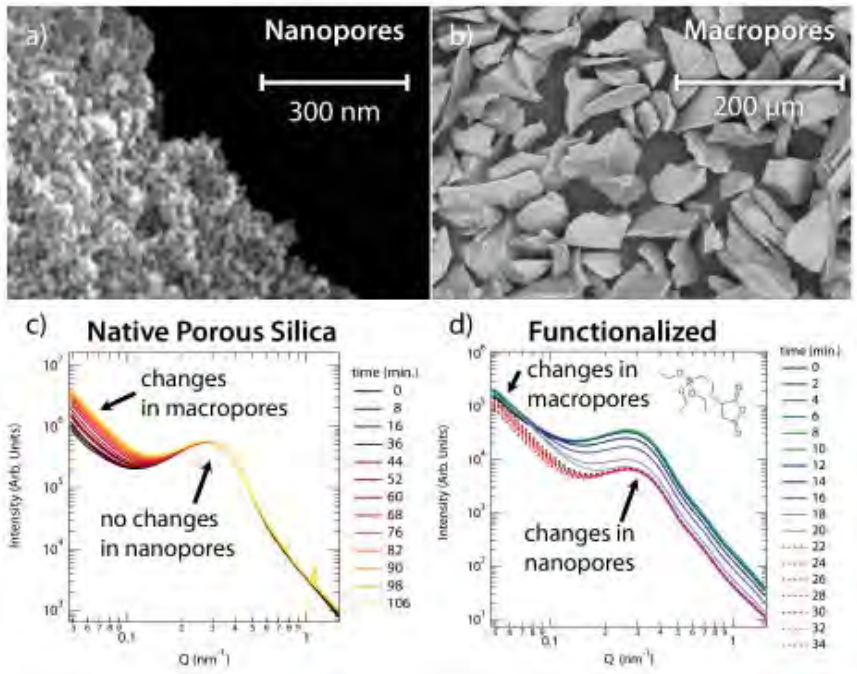

Figure 5. Precipitation of calcium carbonate in controlled pore glass (CPG). a) Each CPG grain consists of amorphous silica filled with nanopores ~7–8 nm in diameter. b) The pore spaces in between grains form pores tens of micrometers in diameter. c) Small Angle X-ray Scattering (SAXS) intensity as a function of momentum transfer, *Q*, while a fluid supersaturated with respect to calcite is flowed past the CPG. The scattering shows large changes at small *Q*, indicating precipitation in the larger intergranular spaces. d) When the CPG is functionalized with a self-assembled monolayer (structure shown in inset), the precipitation behavior changes so that both the nanopores and macropores fill with precipitate. [Used by permission of American Chemical Society, from Stack AG, Fernandez-Martinez A, Allard LF, Bañuelos JL, Rother G, Anovitz LM, Cole DR, Waychunas GA (2014) Pore-size-dependent calcium carbonate precipitation controlled by surface chemistry. *Environmental Science & Technology,* Vol. 48, p. 6177–6183]

(SiO_2), silica overgrowths initially dissolved in an arenite sandstone followed by precipitation in larger pores. This is consistent with an inhibition of precipitation in smaller pores and unstable precipitates in smaller pores. It is to be hoped that these techniques can be used for further, well controlled experiments that will systematically probe precipitation reactions in porous media. The source of the difficultly in interpreting the results of these experiments may be because these samples are natural ones in which multiple processes could be occurring at once, or at least that multiple effects could be the origin of the observed results. This ambiguity makes isolating specific processes and quantifying their effects difficult. However, measurements on idealized samples, while easier to interpret, are not as applicable. Ideally, work on idealized samples would then be compared to measurements on natural samples as a validation.

ATOMIC-SCALE ORIGINS OF A PORE SIZE DEPENDENCE

Substrate and precipitate effects

What kinds of things could happen that would drive a pore-size dependence for precipitation? Initially, one might imagine that the shape of the pore could result in a change in the ability of the substrate to induce nucleation of a precipitate, change the fluid composition

inside a pore, changing the fluid's ability to precipitate material and the ability of the fluid to transport reactants to the site of reaction. Many of these effects have their origin at the atomic-scale. Here these will be discussed and an estimate of the maximum pore size where any effects could be important will be given.

The reactivity of the substrate could change due to strain induced on the reactive sites on the pore wall due to the presence of the pore. That is, by forcing a curved pore wall, or other shape, the reactive sites at the fluid-substrate interface will be strained and this could change their reactivity, particularly towards dissociatively adsorbed water. This in turn would affect their acidity (pK_a), and the surface charge of the substrate would change and the substrate's affinity for dissolved ions that adsorb to nucleate the new phase. There are relatively few direct observations of the acidity of nanopores relative to planar substrates: Fernandez-Martinez (2009) fit the pK_a's of the octahedral aluminum surface sites on nanotubular imogolite ($Al_2SiO_3(OH)_4$) and found they are one pK_a unit more acidic than the equivalent sites on macroscopic gibbsite ($Al(OH)_3$). However, Bourg and Steefel (2012) found that the difference in bond lengths on amorphous silica nanopores translated to only a 0.5-1 pK_a unit difference using classical molecular dynamics simulations. Studies of the charge densities of nanoporous amorphous silica similarly found that silanol functional group densities are within a factor of two of a planar amorphous silica surface. There are 2.5–3 >SiOH groups/nm^2 in a nanoporous amorphous silica, Mobil Composition of Matter No. 41 (MCM-41), versus 5–8 sites per /nm^2 in typical amorphous silica (Sahai and Sverjensky 1997; Zhao et al. 1997).

One strategy to understand the limits on possible effects of pore size on reactivity is to examine structural relaxation of near surface layers on bulk mineral phases and use their typical extent as a measure of the distances over which atomic-level strain is typically dissipated. Molecular simulation and X-ray reflectivity (XR) are the best methods to look at relaxation of a structure at a planar mineral–water interface. These typically show modifications of the average positions of atoms in a few of the top-most monolayers of a crystal surface due to the creation of the interface. For example in the barite {001} surface, in XR experiments (Fenter et al. 2001) and MD simulations (Stack and Rustad 2007), show a bulk-like structure after about three monolayers depth, which is about 1 nanometer (Fenter et al. 2001) (Fig. 6). XR on hematite (α-Fe_2O_3) also shows about three monolayers that relax, or about 0.7 nm (Trainor et al. 2004), and XR/MD on calcite shows about 4 monolayers, or 1.1 nm (Fenter et al. 2013). If we take these measurements as a guide, it suggests that only the very smallest nanopores (less than a few nanometers) should show some change in localized atomic structure due to the presence of the pore and different reactivity. Any larger pores will likely show more or less planar-like reactivity of the substrate. An alternative guide might be taken from measurements on nanoparticles, which might be thought of as nanopores in reverse. Anatase (TiO_2) nanoparticles show bulk-like points of zero charge and protonation constants when particle size is larger than 4 nm in diameter, but smaller than that they start to deviate (Ridley et al. 2013).

Regarding other species besides water, Singer et al. (2014) measured sorption of strontium and uranium in a porous amorphous silica (MCM-41) with pore sizes of 4.7 nm. They found that the presence of the nanopores lead to the uranium and strontium desorption to be recalcitrant relative to bulk silica, i.e., it took a stronger solvent to labilize the uranium ions, but sorption occurred with a lower total adsorption density than the corresponding bulk phases. This was argued to be consistent with results from uranium contaminated-sediments containing a larger fraction of nanopores (Bond et al. 2008). However, as was discussed in the publication, it was not demonstrated that this is due to the reactivity of the pores themselves, but the possibility that the change in reactivity could be due to diffusion of the ions into pores themselves. This demonstrates a pervasive problem in understanding reactivity in pores: how does one separate transport from reactivity effects? In the Stack et al. (2014) study

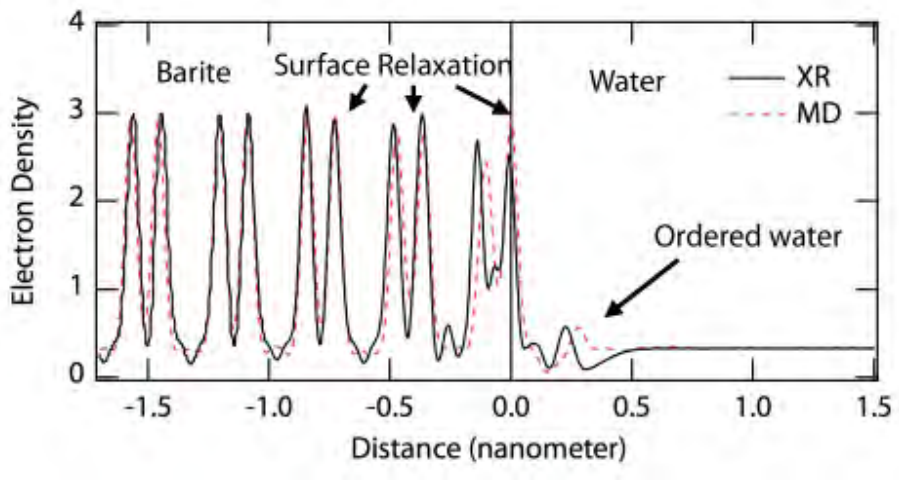

Figure 6. Atomic-scale electron density as a function of distance from a barite {001} mineral–water interface. Barite (negative numbers in *x*-axis) shows surface relaxation on the order of three monolayers. Water (positive numbers in *x*-axis) shows one or more ordered water peaks. Black line is X-ray Reflectivity (from Fenter et al., 2001), dashed line is from Molecular Dynamics (Stack and Rustad 2007). A 5% lattice mismatch has been corrected in the MD data. MD data has been broadened and weighted to atomic number courtesy of Sang Soo Lee (see acknowledgements).

described above, it was observed that neutron scattering originating from the nanopores in the native CPG responded to a solution change as rapidly as new scattering patterns could be measured (~20 min). This was thought to suggest that transport, at least of water, is relatively facile into the nanopores themselves. Additionally, CPG may contain differing reactivity from MCM-41. This is evidenced by SAXS measurements of MCM-41 and another nanoporous amorphous silica (SBA-15) that show dissolution and re-precipitation of silica in water at 60 ºC (Gouze et al. 2014), whereas we have not observed this with CPG (at least, at room temperature and pH ~8.5; Stack et al. 2014).

In order to conceptualize some of how the presence of nanopores can affect precipitation reactions, it is useful to review some of classical nucleation theory (De Yoreo and Vekilov 2003). The free energy of a precipitating phase (ΔG) is the sum of two terms (De Yoreo and Vekilov 2003):

$$\Delta G = \Delta G_{\text{bulk}} + \Delta G_{\text{surface}}, \tag{3}$$

where ΔG_{bulk} is the contribution from the bulk volume of precipitated material and $\Delta G_{\text{surface}}$ is the contribution from the interfacial energy. For a heterogeneous nucleus, the free energy conserved for a given radius is:

$$\Delta G_{\text{bulk}} = -\frac{2\pi r^3 (2.303 \text{k}_\text{B} T \cdot SI)}{3V_m}, \tag{4}$$

where r is the radius of the nucleus, k_B is Boltzmann's constant, T is temperature, SI is saturation index, and V_m is the molar volume (in m^3/mol). Saturation index is defined as the log of the activities of the constituent ions of the mineral divided by the solubility product. For calcite this is $SI = \log(a_{\text{Ca}} a_{\text{CO}_3} / K_{\text{sp}})$. In Figure 4a, this term is calculated for $SI = 0.76$ and molar volume of calcite (3.69×10^{-5} m^3/mol). For heterogeneous nucleation, the surface energy term is (Fig. 4a):

$$\Delta G_{\text{surface}} = \pi r^2 (2\gamma_{\text{lc}} + \gamma_{\text{sc}} - \gamma_{\text{ls}}), \tag{5}$$

where γ_{lc} is the interfacial energy between the precipitating crystal and the surrounding liquid, γ_{sc} is the energy between the substrate and the crystal, and γ_{ls} is that between the substrate and the liquid. The sum of these terms will be referred to as the apparent interfacial energy, γ'. In Figure 4a, this term is calculate using an apparent interfacial energy for calcite of $\gamma' = 0.036$ J/m^2 (Fernandez-Martinez et al. 2013). If a nanopore changes any of the terms in Equations (4) and (5), it would change how favorable nucleation is, and especially what the critical radius of the nucleus is, that is, the minimum size at which subsequent growth of the nucleus is energetically favorable (Fig. 4b). If the precipitate itself is the same as what would form on a planar substrate, ΔG_{bulk} would not change. Within $\Delta G_{surface}$, the interfacial energy between the substrate and liquid might change due to reactivity with respect to water or surface charge changes such as described above. The energy interfacial energy between the substrate and crystal might also change for the same reasons. These effects will in turn affect the critical nucleus size, or alternately, require a different saturation index to create a stable precipitated nucleus (adjusting *SI* in Equation (4) will change critical radius size as well).

An additional possibility is that the close proximity of surface sites could enhance nucleation within a nanopore, even if reactivity of the surface sites is the same. Hedges and Whitelam (2012) ran a series of Ising model simulations to examine how pore geometry can affect nucleation rate. They found that pores of a specific size and shape could lower the free energy barrier to nucleation. This result is rationalized by the following train of logic: When the free energy of the interface between the precipitating phase and the substrate is lower than the free energy between the precipitating phase and the solution, heterogeneous nucleation onto the substrate will occur at a lower supersaturation than precipitation directly from solution. In this scenario, the precipitate nuclei will minimize the amount of surface area contacting solution and maximize the surface area contacting the substrate. If one were to think about this phenomenon in terms of pore size and shape, a particular size and geometry will minimize the amount of precipitate nuclei–solution interface (Fig. 4). For this phenomena to be an accurate description of what is occurring in pores, the size of the nuclei where significant savings in interfacial energy could be achieved will be similar to the size of the critical radius of the nuclei. This is something like a few nanometers or so (see below; Stack et al. 2014), that is, the pore must be a nanopore. Some evidence of this phenomenon has come from monitoring precipitation on planar substrates, where nuclei can be shown to form preferentially on steps on a surface (Stack et al. 2004), which might be thought of as sharing the structural characteristics of the nanopores as conceived of by Hedges and Whitelam (2012). To the contrary, nucleation in the controlled pore glass described above shows inhibited precipitation in nanopores in the native CPG but simultaneous precipitation in nanopores and macropores in the SAM-functionalized CPG. Note that this thought process is only valid when if interfacial energy is limiting the rate of nucleation. If the interfacial energy is a secondary effect because the kinetically viable pathways for precipitation are limited, the geometry of the nanopores may have no effect on nucleation. That is, despite that a reaction may be thermodynamically favorable, if there is no readily available reaction mechanism for that to happen, or if a competing reaction proceeds more rapidly than the most favorable one, it is likely the reaction will proceed to a metastable state rather than equilibrium.

There is an alternate interpretation of the effects of pore size on surface energy. The argument runs that since the presence of the pore artificially limits the size of the nuclei that precipitate inside of them, it increases the proportion of the surface energy relative to the total energy. This is well known from the classical nucleation theory described above, where a critical radius is defined as the radius in which the energy conserved by creating

the volume of the precipitated material is balanced by the energy penalty for creating the surface area of the nuclei-solution interface (Fig. 4b). Thus a smaller nuclei has a greater surface energy and is less stable (according to the theory). If the precipitation occurs, e.g., in a nanopore, the net effect is to increase the apparent solubility of a precipitate of restricted size. Thus, a higher saturation state is required to induce heterogeneous precipitation in the pore than would otherwise be required. This model is called the Pore Controlled Solubility (PCS) model. In its Equation form, it is:

$$S_d = S_0 \exp\left\{\frac{2V_m\gamma}{\mathrm{R}Tr}\right\}, \tag{6}$$

where S_d is the effective saturation state of the fluid inside a pore with respect to a mineral phase, S_0 is the intrinsic saturation state in bulk fluid, V_m is the molar volume of the material (m^3/mol), γ is the interfacial energy of the precipitating phase (J/m^2), R is the ideal gas constant (J/mol/K), T is temperature (K) and r is the radius of the pore (m). The evidence of this effect has been noted in silica aerogel (pore sizes of 100–400 nm) where increased saturation index is required above that normally necessary to nucleate barite (Prieto et al. 1990; Putnis et al. 1995). This effect has also been observed in halite (NaCl) cements in sandstones (Putnis and Mauthe 2001) and in porosity distributions of quartz-cemented sandstone in proximity to a styolite (Emmanuel et al. 2010). In these studies at the micrometer scale, it was found the cements had filled more of the larger pores than the smaller pores, and Putnis and Mauthe (2001) found that the halite was preferentially leached from larger pores. In contrast, Stack et al. (2014) showed that the critical radius of a calcite grain is 1.5 nm using $V_m = 3.69 \times 10^5$ m^3/mol; $\gamma_{sl} = 0.094$ J/m^2 (Stumm and Morgan 1996) using Equation (6) in their system, smaller than the nanopores in the CPG. To put this into perspective, the critical diameter of the nanopore is equivalent to about twice the interlayer of a swelling clay—that is to say, the nuclei in all but the smallest nanopores should be larger than the critical radius of the calcium carbonate. For a pore that is e.g., 8 nm in diameter, the solubility should be increased by a factor of 2.1. This corresponds to a saturation index of 0.3 necessary to make these nuclei stable, which is a minor effect given that $SI = 0$ is equilibrium).

The PCS model of Emmanuel and coworkers and the Ising model of Hedges and Whitelam are directly contradictory. The Ising model says that interfacial energy is reduced in a nanopore, promoting nucleation, whereas PCS says interfacial energy is increased in nanopores, inhibiting nucleation (Fig. 4b). The latter has significant empirical findings that correlate with it, but some of that work is in much larger, micrometer-sized pores, which are in regimes larger than what might be expected for these types of effects. Our work in nanopores has supported the PCS concept in the native CPG grains, but that nucleation can occur in nanopores (Stack et al. 2014). This was thought to occur by lowering the interfacial energy between the substrate and precipitate by introducing a SAM, something not accounted for in the PCS model.

Nucleation density of the precipitate on the substrate may also be important. Using neutron diffraction, Swainson and Schulson (2008) found that ice nucleation in diatomite and chalk was inhibited and proceeded by a small number of nuclei that grew to fill neighboring pores. If nucleation density is low, one might expect what appeared to be a preference for precipitation in large pores, since these pores would contain the largest precipitates. A high nucleation density would appear more like a uniform coating of the substrate.

EFFECTS IN SOLUTION

In all of these studies, there are questions about the role of the composition of fluids. That is, one cannot rule out that the nanopores affect the near surface solution composition and affect the outcome of the precipitation reactions. We know that the presence of pores can induce changes in the structure and ion composition. How large are these effects? To get an idea, we will first examine the classical model of a charged mineral–water interface, a Gouy–Chapman diffuse layer, often coupled to a stern layer that includes discrete dissolved species. These are reviewed extensively in a previous volume of *Reviews in Mineralogy and Geochemistry* (Davis and Kent 1990; Parks 1990). Briefly, the concept is that the presence of the interface creates dissatisfied bonding environments for surface atoms, which leads dissociation of water as it adsorbs onto mineral surface sites whose charge creates an electrical potential that is attracts ions of opposite charge to adsorb onto the mineral surfaces themselves. Ions also collect in an area the electric double layer which extends into the solution until the electrical potential is negated. The extent to which the surface potential decays into the solution diffuse layer is approximately described as:

$$\psi = \psi_0 \exp(-\kappa d) \tag{7}$$

where ψ is the potential at some distance, d, from the surface, ψ_0 is the potential at the surface (or Stern or beta layers if using a two or three layer model), and κ is the Debye parameter:

$$\kappa = \left(\frac{2\mathrm{F}^2 I \times 10^3}{\varepsilon\varepsilon_0 \mathrm{R}T} \right) = 3.29 \times 10^9 \sqrt{I} \quad (\mathrm{m}^{-1}) \tag{8}$$

where F is the Faraday constant (96,485 C/mol), I is the ionic strength (in mol/L), ε is the dielectric constant of water (78.4 at 298 K), ε_0 is the permittivity of a vacuum (8.854×10^{-12} $\mathrm{C}^2/\mathrm{N/m}^2$), R is the ideal gas constant (8.314 J/mol/K) and T is temperature (298 K). We can use the reciprocal of the Debye parameter as an estimate for where the overlap between diffuse layers becomes significant. This "Debye length" is 0.96 nm in solutions with I = 0.1 M electrolyte concentration, 3.1 nm for 0.01 M, and 9.6 nm for 0.001 M electrolyte concentrations (Fig. 7a). In pure water ($I = 10^{-7}$ M), the Debye length is 960 nm. One might expect to observe significant changes in the concentrations of ions when the pore size is decreased sufficiently such that the diffuse layers on either side of the pore start to overlap. If we take the size of the area of significant interaction as roughly twice the Debye length, the pore size ranges from 2 nm up to nearly 2 μm in pure water depending on ionic strength. In concentrated solutions, the size of the pores where one would expect to observe electrolyte effects is quite small, basically the lower limit on the size of a nanopore. In the extreme case of dilute water however, this theory predicts that the pore sizes where electric double layer effects would be seen could be substantial. In natural systems pure water is not reasonably expected to be observed, but in experiments researchers will sometimes minimize the ionic strength since the composition and concentration of the electrolyte affects mineral precipitation reaction mechanisms and rates (e.g., Ruiz-Agudo et al. 2011; Kubicki et al. 2012; Bracco et al. 2013).

Within the electric double layer, one would see elevated concentrations of the ions that are oppositely charged to the mineral surface and lower concentrations of the ions that are of the same charge. For example, at pH 7 in 0.1 M NaCl, amorphous silica is negatively charged (Sahai and Sverjensky 1997; Sverjensky 2006), so one would expect an excess of sodium cations and decreased amounts of chloride. This is significant in that differences in the reactivity of precipitation rates have been observed, depending on the cation-to-anion ratio of the solution. For example, with calcium carbonate, the calcium-to-carbonate ratio

affects whether growth is observed at all (Stack and Grantham 2010), as well as whether growth proceeds through homogeneous nucleation directly from solution, or growth by pre-existing seed crystals (De Yoreo and Vekilov 2003; Gebrehiwet et al. 2012; Stack 2014). How elevated/depleted could concentrations be inside a nanopore? Using the electric double layer formulation again to examine concentration of dissolved electrolyte:

$$c_+ = c_\infty \exp\left(\frac{-zF\psi}{RT}\right) \quad c_- = c_\infty \exp\left(\frac{zF\psi}{RT}\right) \tag{9}$$

where c_+ and c_- are the concentrations of cations (c_+) and anions (c_-) within the electric double layer, c_∞ is the concentration of that ion in bulk solution, z is the charge on the ion, and all the other symbols are defined above. Using this, we can say that if the surface potential is -50 mV and a monovalent cation concentration is 0.01 M, then the concentration of the cation at the surface is nearly 7× the bulk concentration (c_+/c_∞). This is substantial enough to make a large difference in if precipitation occurs or not (Fig. 7). This may not be valid however, since the diffuse layer model breaks down very close to the interface (see below). If the calculation is done at some distance from the mineral–fluid interface, e.g., at the Debye length (3.1 nm; Eqn. 5), the potential is -18 mV (Eqn. 4) and a diffuse layer concentration is therefore 2× the bulk concentration (Eqn. 6). This is much less significant and will not affect rates nearly as strongly, but the cation-to-anion ratio will still change by a factor of four.

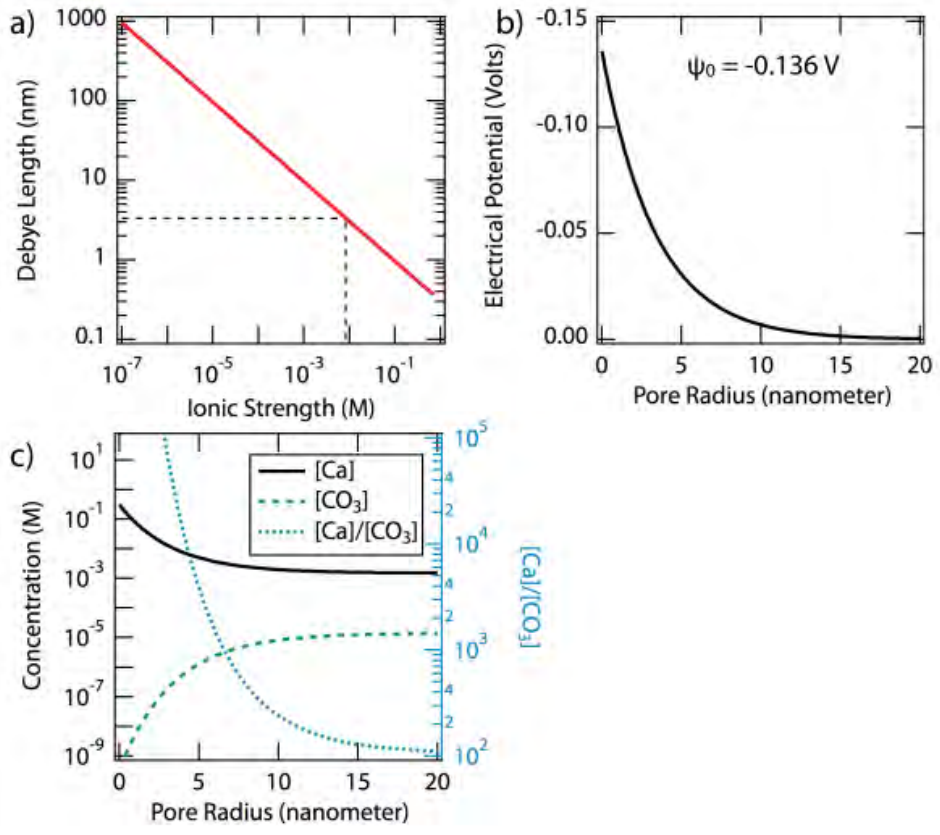

Figure 7. Electric double layer (EDL) effects within a pore. a) Debye length, or double-layer thickness, as a function of ionic strength. Dashed lines are the example used to examine the data in Figure 5. b) Electrical potential decaying into solution for the ionic strength highlighed in a. c) Change in concentrations of calcium and carbonate (left axis) due to EDL as a function of distance from the pore wall. The right axis shows the aqueous calcium-to-carbonate ratio, which reaches extreme values closer to the pore wall as small radii.

As a real world example of how the electric double layer may affect the concentrations of ions in nanopores, it can be applied to explain, perhaps, the results of Figure 5. Specifically, Stack and Grantham (2010) and Gebrehiwet et al. (2012) have shown that calcite growth rate depends in part on the calcium-to-carbonate ratio, so if the CPG in Stack et al. (2014) had significant surface charge, it could affect not just rate of precipitation, but even if it occurs or not. The ionic strength of the solution used in the experiments in Figure 5 was 8.2×10^{-3} M, whose constituent ions consist of chloride, calcium, sodium, carbonate and bicarbonate. Using Equation (8), the Debye length would be 3.3 nm, so we would expect a pore size dependence at 6.6-nm pore diameter (Fig. 7a), which is close to the fitted size of the pores, 6.9 nm. We would therefore expect that the nanopores would contain significant double layer effects that change the concentration of ions within the pores. The pH of the solution used is ~8.4, which would correspond a surface potential of -136 mV using a Stern–Graham model for silica that includes specific adsorption of calcium ions to surface sites (Sverjensky 2006). We therefore might expect substantial excess calcium adsorbed in the pore walls and within the pores and depleted carbonate and bicarbonate in those same areas. Using Equation (9) and a surface potential of -136 mV for amorphous silica leads to 6.5 × aqueous calcium concentration and 0.024 × carbonate concentration in the center of the pore. This creates an aqueous calcium-to-carbonate ratio at the center of the pore of 29,000 (using a 6.9-nm diameter pore), whereas in the bulk solution it is 107 (Fig. 7c). It is therefore conceivable that such a high calcium-to-carbonate ratio suppresses nucleation (Fig. 8). One caution is that Gebrehiwet et al. (2012) saw enhanced nucleation at calcium-to-carbonate ratios near 300, but Stack and Grantham (2010) saw reduced growth rates of single crystals at high calcium-to-carbonate ratios. The trend observed in Figure 5 is not consistent with increased nucleation rate, but it is conceivable that at such a high calcium-to-carbonate ratio, particularly close to the pore wall where the calcium-to-carbonate ratio would be expected to be more extreme than even in the center of the pore. In this scenario, the reason as to why the self assembled monolayer enhanced nucleation is that it modified the surface so it

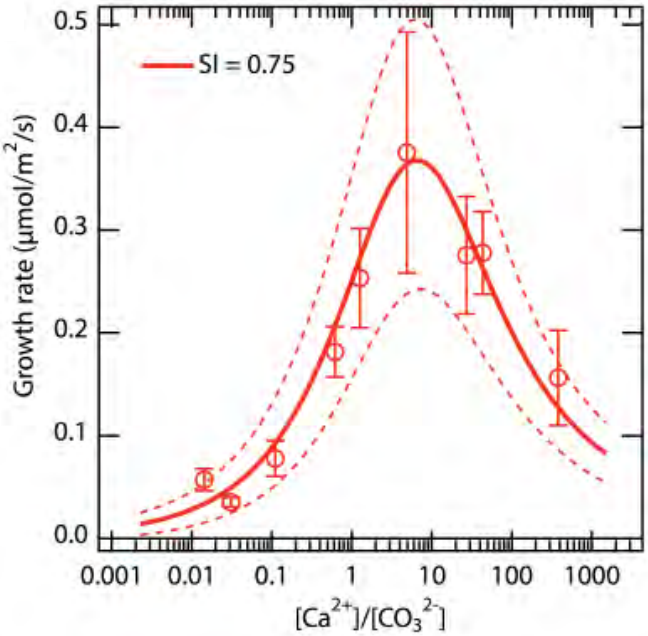

Figure 8. Variation of growth rate of calcite with aqueous calcium-to-carbonate ratio. The peak rate occurs at some ratio slightly greater than one, but decreases substantially at ratios far from that. [Used by permission of John Wiley & Sons, from Stack AG (2014) Next-generation models of carbonate mineral growth and dissolution. *Greenhouse Gas Science & Technology,* Vol 4, p. 278–288]"

contained a smaller surface charge than the native silica, or perhaps had not yet hydrolyzed to form a dicarboxylic acid (while surface charges were not measured in those experiments, the functionalized CPG was observed to clump more readily than the original material, suggesting that there may have been difference in surface charge). A smaller surface charge might allow the nanopore solution composition to reflect that of the bulk solution and create an environment more favorable for nucleation.

One persistent doubt that remains is the physical plausibility of the electric double layer concept at the atomic scale. It is well known that the diffuse layer model alone overestimates concentrations at high concentrations, a failing which can be corrected by use of one or more Stern–Graham layers that accounts for adsorption of ions into planes of fixed height and capacitance (e.g., Davis and Kent 1990). However, recent evidence has suggested that the capacitance and thickness of a Stern–Graham layer are not necessarily constants, but vary with solution composition (Pařez and Předota 2012) and especially close to an interface (Pařez et al. 2014). A more difficult problem is that direct measurements of mineral–water interface structure using X-ray Reflectivity (XR) and Resonant Anomalous X-ray Reflectivity (RAXR) (Lee et al. 2010; Fenter and Lee 2014) have not shown increased concentrations of ions more than ~3 nm from an interface (Fig. 9). Distributions of ions that it does show tend to be localized in inner-sphere, outer-sphere or extended outer-sphere complexes and not a smoothly decaying concentration gradient as expected from the diffuse layer concept in

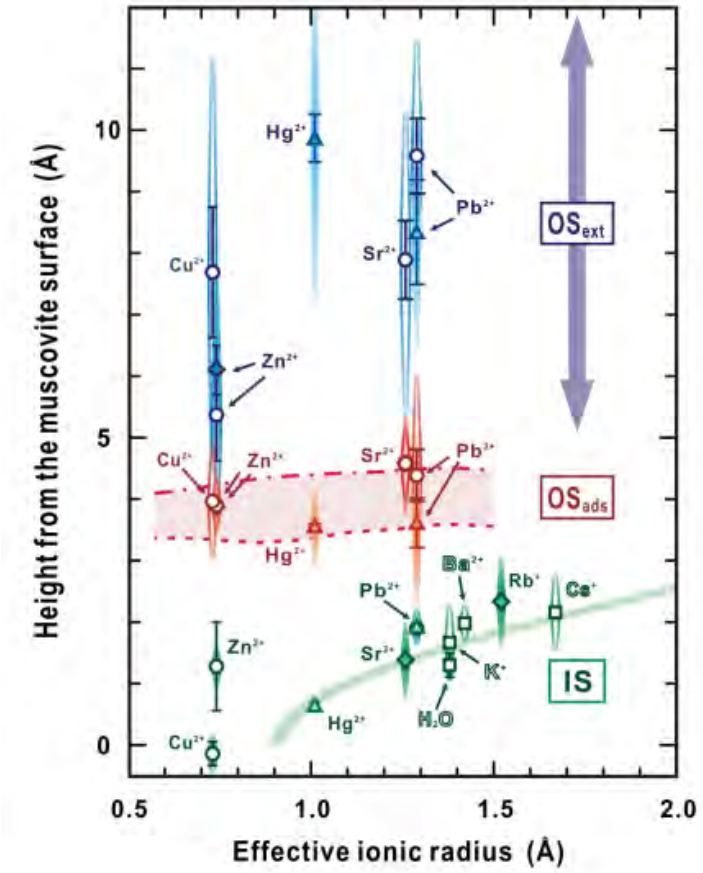

Figure 9. Average heights of distributions of ions adsorbed to a muscovite mica surface, measured using Resonant Anomalous X-ray Reflectivity. IS is inner-sphere, OS_{ads} is outer-sphere and OS_{ext} is an extended out-sphere complex. [Used by permission of the American Chemical Society, from Lee SS, Fenter P, Park C, Sturchio NC, Nagy NL (2010) Hydrated cation speciation at the muscovite (001)-water interface. *Langmuir,* Vol. 26, p. 16647–16651]

Equation (7). This discrepancy may arise from a couple of possibilities, such as the detection limit of ions using the XR and RAXR techniques, and the fact that a fitted adsorption profile is not necessarily a unique fit to the scattering data. There is some recent evidence from molecular dynamics simulations that the assumption of a dielectric "constant" breaks down at the molecular level for a charged interface and that the effective dielectric constant can oscillate wildly depending on local water ordering and that this strongly affects decay of electrical potential into solution (Pařez et al. 2014). Typically in MD simulations ordered water is also observed less than one nanometer from the surface (Fig. 6) (Stack and Rustad 2007; Bourg and Sposito 2011; Fenter et al. 2013). This is consistent with the XR, although these two techniques are seldom in perfect agreement, likely stemming from the uncertainty in the MD models in addition to those of the XR. If one uses these more recent observations as a limit to what sized pores interfacial regions would start to overlap, the answer is much smaller than using the classical electric double layer.

TRANSPORT

The last subject that will be addressed here is that of transport. This is the subject of other articles in this volume (Steefel et al. 2015, this volume), so this discussion will only revolve around those aspects that specifically involve precipitation. The classical concept for precipitation reactions is that they are either surface chemistry controlled or transport controlled, depending on the mixing rate of the solution. For example, Plummer et al. (1978) found that below pH ~5.0, the dissolution rate of calcite depended on how rapidly an impellor stirred the solution in the reactor. This is quantified as the Damköhler number, which is the reaction rate divided by the convective mass transport rate (Fogler 2006). In a natural porous system, i.e., in groundwater, it is not clear if sufficiently high flow rates are ever reached to make the system entirely free of a transport constraint. This was demonstrated recently by Molins et al. (2012) who showed the dissolution rate of calcite as a function of darcy velocity, or net fluid velocity (Fig. 10). Molins et al. (2012) show that the transition from a transport-limited to a surface chemistry-limited reaction is not sharp, but is a gradient. Furthermore,

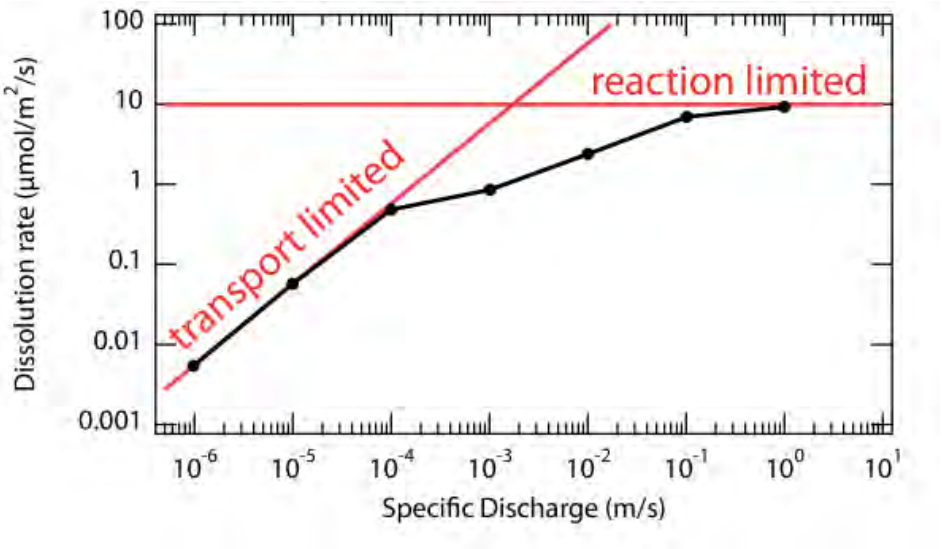

Figure 10. Dissolution rate of calcite as a function of specific discharge (velocity). As the solution moves through the porous medium more quickly, transport of the fluid plays more of a role in determining the rate of reaction, but there is a broad range of flow velocities where the rate is transport limited in some pores, but limited by reaction kinetics in others. Adapted from Molins et al. (2012).

they observed that the volume-averaged rate of dissolution was slower than the open solution rate because not all pores had the same fluid velocities. Liu et al. (2013) also found that while chemical reactions may be quite rapid on the near atomic scale, once the tortuous nature of diffusion in a porous system is accounted for, the apparent rate of diffusion is much slower. This is not an insignificant effect: the difference between the microscopic rates of adsorption/desorption or diffusion and the pore- or even grain-scale rates are many orders of magnitude (Liu et al. 2013). Reeves and Rothman (2012) also addressed this issue by highlighting the need for functions for chemical reactivity that scale with time and length.

We also know that for precipitation reactions, the rate of reaction in these systems cannot be described accurately using a single rate constant if solution composition and precipitate surface site concentration vary: one should fit rates using rate constants that reflect the mechanisms of attachment and detachment of ions to known surface sites on the growing crystals, that is, use a kinetics model that reflects the chemical processes observed to occur on a mineral surface (Stack 2014). The rate constants and mechanism for attachment of these ions vary depending on the ion and the mineral. For example, the rate constants for attachment of calcium and carbonate to calcite are ~6.7×10^6 s^{-1} and 3.6×10^7 s^{-1} (Bracco et al. 2013), whereas those for attachment of magnesium and carbonate ions to magnesite ($MgCO_3$) are 4.0×10^5 s^{-1} and 2.0×10^6 s^{-1} (Bracco et al. 2014). From this, one would expect that the zone over which surface kinetics and transport are both important depends not just on the flow rate and the reactivity of the mineral, but the identity of the constituent ions will affect how much of a reaction is transport controlled. That is, for calcite growth one would expect that one could have a condition where calcium attachment is surface-kinetics-limited and carbonate is transport-limited. Due to the relatively small difference in rate constants in these systems, the range of solution conditions over which this might exist is limited but this may not always be true. In fact, mineral growth kinetics measurements such as these may actually reflect this condition already since possible transport limits are often poorly controlled or verified; in Bracco et al. (2012), the step velocity was measured as a function of flow rate under one condition, but not under all calcium-to-carbonate ratios so the rate constant for carbonate quoted above may reflect a partial transport control over carbonate attachment.

Another significant issue due to transport effects are due to the mixing of solutions. Because the grid cell size used in conventional reactive transport models is larger than the scale over which precipitation is typically observed, they have a tendency to overestimate the amount of fluid mixing and precipitation. In Tartakovsky et al. (2008) and Yoon et al. (2012), the precipitation of calcium carbonate phases was observed and modeled in a sand-packed reactor where solutions of dissolved $CaCl_2$ and Na_2CO_3 were injected along parallel flowpaths. They observed precipitation where the two streams mixed, but at a much finer scale than what would have been captured by a conventional grid-cell approach (Fig. 11a). They found that a smoothed-particle hydrodynamic model was able to capture the localization of the precipitation reaction well (Fig. 11b), or additionally a Darcy-type simulation with smaller grid sizes in the zone where precipitation was observed also was accurate. These studies highlight an ongoing research problem, which is how create a model that scales dynamically to capture the microscopic reactions well, but also is practical to use at much larger scales. One is not able run the molecular dynamics simulation over an entire reservoir or watershed, and never will be, so models that can capture atomic-scale reactions well, but also scale upwards in time and space, are necessary. As mentioned in the discussion above, Tartakovsky et al. (2008) found that the relationship between porosity and permeability is not as straightforward as it may seem in that the precipitation could create an impermeable barrier at only a 5% reduction in porosity. This result demonstrates that empirical relationships between porosity and permeability built from analysis of natural samples will not necessarily be applicable to anthropogenically induced precipitation. Lastly, one must also account for dissolution. During

the mixing experiments just described, the sequence of events is that as the two solutions mix, they become saturated and eventually supersaturated sufficiently for precipitation to become favorable. Precipitation occurs and blocks communication between the two mixed fluids. Once the mixing is shut down, the solution surrounding the precipitate is then undersaturated and the precipitate should start to dissolve. Yoon et al. (2012) found that while they could model the precipitation relatively well by adjusting conventional precipitation models (Chou et al. 1989), but the subsequent dissolution was not well captured.

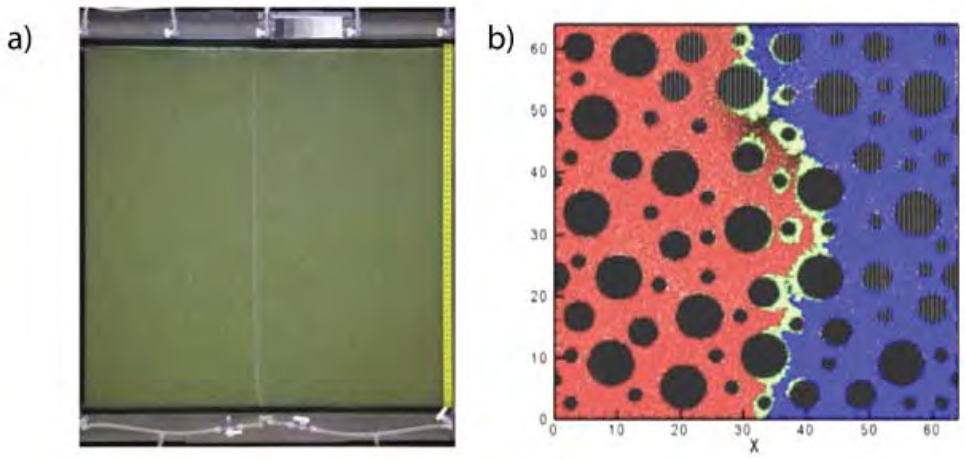

Figure 11. Calcium carbonate precipitation in a sand-packed reactor. Two solutions, $CaCl_2$ and Na_2CO_3 are circulated side-by-side. a) Photograph of results; the white vertical stripe is a thin layer of calcium carbonate phases that have precipitated. b) Smoothed Particle Hydrodynamic model results that captures the localized nature of the precipitation well. The green (lighter gray) color shows the precipitated material. Red (left) and blue (right) are the two different injected solutions. [Used by permission of John Wiley & Sons, from Tartatakovsky AM, Redden G, Lichtner PC, Scheibe TD, Meakin P (2008) Mixing-induced precipitation: Experimental study and multiscale numerical analysis. *Water Resources Research,* Vol. 44, W06S04]

CONCLUSIONS AND OUTLOOK

From these studies, it is clear that precipitation within a porous medium is a complex process that is a challenge to observe and model accurately and even in idealized systems, there are multiple effects that potentially explain the results. One must consider mineral precipitation kinetics (which are very complex themselves), substrate reactivity, surface charges and ion adsorption affinities that are possibly different from the bulk phase, geometric factors that inhibit or enhance nucleation, surface energy effects, and last but not least, solvent transport. In natural systems multiple minerals and other phases (such as organic carbon), gradients in pore size distributions and other components create potentially other complicating factors that reduce our ability to discern what is occurring in these systems. Nanopores may contain the largest deviations from bulk-like reactivity, and at the same, may constitute the majority of pores in a rock. Yet, due to the difficulty in quantitatively measuring these, the relative importance of nanopores to the net reactivity of the rock, and their reactivity in this context are just beginning to be examined. The precipitation itself is fairly difficult to observe since it is occurring in the middle of three dimensional network of solids, leaving one to either interpret data from thin sections or utilize newer methods of X-ray and neutron scattering that can allow one to gather statistical averages of the porosity distribution. To interpret and understand how the presence of a porous medium affects mineral precipitation will find application in multiple areas of scientific, environmental and industrial interest. These include metal contaminant treatment, carbon sequestration, scale formation, mineral/rock weathering, perhaps seismicity,

etc. The potential to examine reactivity in pores is positive, however, in that new experimental probes such as X-ray and neutron scattering are being adapted to probe these reactivity in porous media, and coupled enhanced reactive transport modeling capabilities. Understanding derived from these combined methods may result in predictive theories that can accurately account for atomic-scale reactivity and structure, but are useful at larger scales where it is no longer practical to resolve individual pores.

ACKNOWLEDGMENTS

The author wishes to thank both Sang Soo Lee at Argonne National Laboratory for his translation of the MD probability curves to be more comparable to the XR (Fig. 6), and Michael L. Machesky of the Illinois State Water Survey for sanity-checking the calculations of the surface potential of amorphous silica (Fig. 7). Research on CO_2 sequestration sponsored by the Center for Nanoscale Control of Geologic CO_2, an Energy Frontier Research Center funded by the U.S. Department of Energy, Office of Science, Office of Basic Energy Sciences under Award Number (DE-AC02-05CH11231). Research on barite and metal contaminants was supported by the U.S. Department of Energy, Office of Science, Basic Energy Sciences, Chemical Sciences, Geosciences, and Biosciences Division. The author is grateful for the insightful comments by Alejandro Fernandez-Martinez and Qingyun Li that significantly improved the manuscript.

REFERENCES

Anovitz LM, Cole DR (2015) Characterization and analysis of porosity and pore structures. Rev Mineral Geochem 80:61–164

Anovitz LM, Cole DR, Rother G, Allard LF, Jackson AJ, Littrel KC (2013) Diagenetic changes in macro- to nano-scale porosity in the St. Peter Sandstone: An (ultra) small angle neutron scattering and backscattered electron imaging analysis. Geochim Cosmochim Acta 102:280–305

Arey JS, Seaman JC, Bertsch PM (1999) Immobilization of uranium in contaminated sediments by hydroxyapatite addition. Environ Sci Technol 33:337–342

Beazley MJ, Martinez RJ, Sobecky PA, Webb SM, Taillefert M (2007) Uranium biomineralization as a result of bacterial phosphatase activity: insights from bacterial isolates from a contaminated subsurface. Environ Sci Technol 41:5701–5707

Berner RA, Lasaga AC, Garrels RM (1983) The carbonate-silicate geochemical cycle and its effect on atmospheric carbon dioxide over the past 100 million years. Am J Sci 283:641–683

Bethke CM (1986) Inverse hydrologic analysis of the distribution and origin of Gulf Coast-type geopressured zones. J Geophy Res 91:6535–6545

Bleam WF (2011) Soil and Environmental Chemistry. Academic Press, Amsterdam.

Bloch S (1991) Empirical prediction of porosity and permeability in sandstones. Am Assoc Pet Geol Bull 75:1145–1160

Boerner LK (2013) Sewage plants struggle to treat wastewater produced by fracking operations. Chemical & Engineering News, March 18, 2013

Bond DL, Davis JA, Zachara JM (2008) Uranium(VI) release from contaminated vadose zone sediments: estimation of potential contributions from dissolution and desorption. *In*: Barnett, MO, Kent, DB (eds), Adsorption of Metals by Geomedia II. Academic Press, San Diego, CA, p 379–420

Borgia A, Pruess K, Kneafsey TJ, Oldenburg CM, Pan L (2012) Numerical simulation of salt precipitation in the fractures of a CO_2-enhanced geothermal system. Geothermics 44:13–22

Bourg IC, Sposito G (2011) Molecular dynamics simulations of the electrical double layer on smectite surfaces contacting concentrated mixed electrolyte (NaCl–$CaCl_2$) solutions. J Coll Int Sci 360:701–715

Bourg IC, Steefel C (2012) Molecular dynamics simulations of water structure and diffusion in silica nanopores. J Phys Chem C 116:11556–11564

Bracco JN, Grantham MC, Stack AG (2012) Calcite growth rates as a function of aqueous calcium-to-carbonate ratio, saturation index, and inhibitor concentration: Insight into the mechanism of reaction and poisoning by strontium. Cryst Growth Des 12:3540–3548

Bracco JN, Stack AG, Steefel CI (2013) Upscaling calcite growth rates from the mesoscale to the macroscale. Environ Sci Technol 47:7555–7562

Bracco JN, Stack AG, Higgins SR (2014) Magnesite step growth rates as a function of the aqueous magnesium:carbonate ratio. Cryst Growth Des 14:6033–6040

Carey, JW (2013) Geochemistry of wellbore integrity in CO_2 sequestration: Portland cement-steel-brine-CO_2 interactions. Rev Mineral Geochem 77:505–539

Chen Y, Wei L, Mastalerz M, Schimmelmann A (2015) The effect of analytical particle size on gas adsorption porosimetry of shale. Intl J Coal Geol. 138:103–112

Chou L, Garrels RM, Wollast R (1989) Comparative study of the kinetics and mechanisms of dissolution of carbonate minerals. Chem Geol 78:269–282

Cohen Y, Rothman DH (2015) Mechanisms for mechanical trapping of geologically sequestered carbon dioxide. Proc. R. Soc. A 471:2010853

Curti E, Fujiwara K, Iijima K, Tits J, Cuesta C, Kitamura A, Glaus MA, Müller W (2010) Radium uptake during barite recrystallization at 23 ± 2 ºC as a function of solution composition: An experimental ^{133}Ba and ^{226}Ra tracer study. Geochim Cosmochim Acta 74:3553–3570

Davis, JA, Kent DB (1990) Surface complexation modeling in aqueous geochemistry. Rev Mineral 23:177–260

De Yoreo JJ, Vekilov PG (2003) Principles of Crystal Nucleation and Growth. Rev Mineral Geochem 54:57–93

Drever JI, Clow DW (1995) Weathering rates in catchments. Rev Mineral 31:463–483

Emmanuel S, Ague JJ (2009) Modeling the impact of nano-pores on mineralization in sedimentary rocks. Water Resour Res 45:W04406

Emmanuel S, Anovitz LM, Day-Stirrat RJ (2015) Effects of coupled chemo-mechanical processes on the evolution of pore-size distributions in geological media. Rev Mineral Geochem 80:45-60

Emmanuel S, Ague JJ, Walderhaug O (2010) Interfacial energy effects and the evolution of pore size distributions during quartz precipitation in sandstone. Geochim Cosmochim Acta 74:3539–3552

Fanizza MF, Yoon H, Zhang C, Oostrom M, Wietsma TW, Hess NJ, Bowden ME, Strathmann TJ, Finneran KT, Werth CJ (2013) Pore-scale evaluation of uranyl phosphate precipitation in a model groundwater system. Water Resour Res 49:874–890

Fenter P, Lee SS (2014) Hydration Layer Structure at Solid–Water Interfaces. MRS Bulletin 39:1056–1061

Fenter P, McBride MT, Srajer G, Sturchio NC, Bosbach D (2001) Structure of Barite (001)- and (210)-Water Interfaces. J Phys Chem B 105:8112–8119

Fenter P, Kerisit S, Raiteri P, Gale JD (2013) Is the Calcite-Water Interface Understood? Direct Comparisons of Molecular Dynamics Simulations with Specular X-ray Reflectivity Data. J Phys Chem C 117:5028–5042

Fernández-Martinez A (2009) Physics of natural nanoparticles – water interfaces: chemical reactivity and environmental implications. PhD Dissertation, Observatoire de Grenoble et Laboratoire de Géophysique Interne et Tectonophysique, Grenoble, France

Fernández-Martinez A, Hu Y, Lee B, Jun Y-S, Waychunas GA (2013) In situ determination of interfacial energies between heterogeneously nucleated $CaCO_3$ and quartz substrates: Thermodynamics of CO_2 mineral trapping. Environ Sci Technol 47:102–109

Ferrar KJ, Michanowicz DR, Christen CL, Mulcahy N, Malone SL, Sharma RK (2013) Assessment of effluent contaminants from three facilities discharging marcellus shale wastewater to surface waters in Pennsylvania. Environ Sci Technol 47:3472–3481

Fogler S (2006). Elements of Chemical Reaction Engineering (4th ed.). Pearson Education, Upper Saddle River, NJ.

Fountain H (2015) Turning carbon dioxide into rock, and burying it. New York Times, February 9th, 2015.

Freeze RA, Cherry JA (1979) Groundwater. Prentice Hall, Englewood Cliffs, NJ. p 604

Frenier WW, Ziauddin M (2008) Formation, removal, and inhibition of inorganic scale in the oilfield environment. Society for Petroleum Engineers, Richardson, TX.

Funk J (2014) Ohio acknowledges connection between hydraulic fracturing and Youngstown quakes, will require seismic testing near known fault lines. The Plain Dealer, April 11th, 2014.

Hedges LO, Whitelam S (2012) Nucleation barriers in the Ising model suggest a strategy for patterning a surface to maximally enhance nucleation. Soft Matter 8:8624–8635

Gebrehiwet TA, Redden GD, Fujita Y, Beig MS, Smith RW (2012) The effect of the CO_3^{2-} to Ca^{2+} ion activity ratio on calcite precipitation kinetics and Sr^{2+} partitioning. Geochem Trans 13:1

Gibson-Poole CM, Svendsen L, Underschultz J, Watson MN, Ennis-King J, van Ruth PJ, Nelson EJ, Daniel RF, Cinar Y (2008) Site characterisation of a basin-scale CO_2 geological storage system: Gippsland Basin, southeast Australia. Environ Geol 54:1583–1606

Giesche H (2006) Mercury porosimetry: a general (practical) overview. Part Part Syst Charact 23:9–19

Godinho JRA, Stack AG (2015) Growth kinetics and morphology of barite crystals derived from face-specific growth rates. Cryst Growth Des 15:2064–2071 doi: 10.1021/cg501507p

Gouze B, Cambedouzou J, Parres-Maynadie S, Rébiscoul, D (2014) How hexagonal mesoporous silica evolves in water on short and long term: Role of pore size and silica wall porosity. Microporous Mesoporous Mater. 183:168-176

Hedges LO, Whitelam S (2012) Patterning a surface so as to speed nucleation from solution. Soft Matter 8:8624-8635

Jamtveit, B, Kobchenko M, Austrheim H, Malthe-Sørensen A, Røyne A, Svensen H (2011) Porosity evolution and crystallization-driven fragmentation during weathering of andesite. J Geophys Res 116:B12204

Kubicki JD, Sofo JO, Skelton AA, Bandura AV (2012) A New hypothesis for the dissolution mechanism of silicates. J Phys Chem C 116:17479–17491

Lee SS, Fenter P, Park C, Sturchio NC, Nagy NL (2010) Hydrated cation speciation at the muscovite (001)-water interface. Langmuir 26:16647–16651

Liu C, Shang J, Kerisit S, Zachara JM, Zhu W (2013) Scale-dependent rates of uranyl surface complexation reaction in sediments. Geochim Cosmochim Acta 105:326–341

Maher K, Steefel CI, White AF, Stonestrom DA (2009) The role of reaction affinity and secondary minerals in regulating chemical weathering rates at the Santa Cruz Soil Chronosequence, California. Geochim Cosmochim Acta 73:2804–2831

Martin AJ, Crusius J, McNee JJ, Yanful EK (2003) The mobility of radium-226 and trace metals in pre-oxidized subaqueous uranium mill tailings. Appl Geochem 18:1095-1110.

Melcer A, Gerrish HW (1996) Effects of formation damage on injection operations and on pressure transient tests. *In:* Deep Injection Disposal of Hazardous and Industrial Waste; Apps JA, Tsang C (eds) Academic Press: San Diego, CA, p 277–286

Metz B, Davidson O, de Coninck H, Loos M, Meyer L (2005) IPCC Special Report on Carbon Dioxide Capture and Storage. Cambridge University Press: Cambridge, U.K.

Mito S, Xue Z, Ohsumi T (2008) Case study of geochemical reactions at the Nagaoka CO_2 injection site, Japan. Int J Greenh Gas Control 2:309–318

Molins S, Trebotich D, Steefel CI, Shen C (2012) An investigation of the effect of pore scale flow on average geochemical reaction rates using direct numerical simulation. Water Resour Res 48:W03527

Morse JW, Zullig JJ, Bernstein LD, Millero FJ, Milne P, Mucci A, Choppin GR, (1985) Chemistry of calcium carbonate-rich shallow water sediments in the Bahamas. Am J Sci 285:147–185

Naftz DL, Feltcorn EM, Fuller CC, Wilhelm RG, Davis JA, Morrison SJ, Freethey GW, Piana MJ, Rowland RC, Blue JE (1998) Field demonstration of permeable reactive barriers to remove dissolved uranium from groundwater, Fry Canyon, Utah. EPA Report 402-C-00-001

Pařez S, Předota M (2012) Determination of the distance-dependent viscosity of mixtures in parallel slabs using non-equilibrium molecular dynamics. Phys Chem Chem Phys 14:3640–3650

Pařez S, Předota M, Machesky M (2014) Dielectric properties of water at rutile and graphite surfaces: effect of molecular structure. J Phys Chem C 118:4818–4834

Parks GA (1990) Surface Energy and Adsorption at Mineral/Water Interfaces: An Introduction. Rev Mineral 23:133–176

Plummer LN, Wigley TML, Parkhurst DL (1978) The kinetics of calcite dissolution in CO_2-water systems at 5° to 60 ºC and 0.0 to 1.0 atm CO_2. Am J Sci 278:179–216

Pontbriand CW, Sohn RA (2014) Microearthquake evidence for reaction-driven cracking within the Trans-Atlantic Geotraverse active hydrothermal deposit. J. Geophys Res Solid Earth 119:822–839

Prieto M, Putnis A, Fernandez-Diaz L (1990) Factors controlling the kinetics of crystallization: supersaturation evolution in a porous medium. Application to barite crystallization. Geol Mag 6:485–495

Putnis A, Mauthe G (2001) The effect of pore size on cementation in porous rocks. Geofluids 1:37–41

Putnis A, Prieto M, Fernandez-Diaz L (1995) Fluid supersaturation and crystallization in porous media. Geol Mag 1:1–13

Reeves D, Rothman DH (2012) Impact of structured heterogeneities on reactive two-phase porous flow. Phys Rev E 86:031120

Ridley MK, Machesky ML, Kubicki JD (2013) Anatase nanoparticle surface reactivity in NaCl media: A CD–MUSIC model interpretation of combined experimental and Density Functional Theory studies. Langmuir 29:8572–8583

Riley RG, Zachara JM, Wobber FJ (1992) Chemical Contaminants on DOE Lands and Selection of Contaminant Mixtures for Subsurface Science Research. U.S. Department of Energy, DOE/ER--0547T DE92 014826

Ruiz-Agudo E, Putnis CV, Wang L, Putnis A (2011) Specific effects of background electrolytes on the kinetics of step propagation during calcite growth. Geochim Cosmochim Acta 75:3803-3814

Sahai N, Sverjensky DA (1997) Evaluation of internally consistent parameters for the triple-layer model by the systematic analysis of oxide surface titration data. Geochim Cosmochim Acta 61:2801-2826

Scherer GW (1999) Crystallization in Pores. Cem Concr Res 29:1347–1358

Singer DM, Guo H, Davis JA (2014) U(VI) and Sr(II) batch sorption and diffusion kinetics into mesoporous silica (MCM-41). Chem Geol 390:152–163

Skoumal RJ, Budzinski MR, Currie BS (2015) Earthquakes induced by hydraulic fracturing in Poland Township, Ohio. Bull Seismol Soc Am, doi: 10.1785/0120140168

Stack AG (2014) Next generation models of carbonate mineral growth and dissolution. Greenhouse Gas Sci Technol 4:278–288
Stack AG, Rustad JR (2007) Structure and Dynamics of Water on Aqueous Barium Ion and the {001} Barite Surface. J Phys Chem C 111:16387–16391
Stack AG, Grantham M (2010) Growth rate of calcite steps as a function of aqueous calcium-to-carbonate ratio: Independent attachment and detachment of calcium and carbonate ions. Cryst Growth Des 10:1409–1413
Stack AG, Kent PRC (2015) Geochemical reaction mechanism discovery from molecular simulation. Environ Chem 12:20–32
Stack AG, Erni R, Browning ND, Casey WH (2004) Pyromorphoite growth on lead-sulfide surfaces. Environ Sci Technol 38:5529–5534
Stack AG, Fernandez-Martinez A, Allard LF, Bañuelos JL, Rother G, Anovitz LM, Cole DR, Waychunas GA (2014) Pore-size- dependent calcium carbonate precipitation controlled by surface chemistry. Environ Sci Technol 48:6177–6183
Steefel CI, Druhan JL, Maher K (2014) Modeling coupled chemical and isotopic equilibration rates. Proc Earth Planet Sci 10:208–217
Steefel CI, Beckingham LE, Landrot G (2015) Micro-Continuum Approaches for Modeling Pore-Scale Geochemical Processes. Rev Mineral Geochem 80:217–246
Stumm W, Morgan JJ (1996) Aquatic Chemistry, Chemical Equilibria and Rates in Natural Waters. John Wiley and Sons, Inc., New York.
Sverjensky DA (2006) Prediction of the speciation of alkaline earths adsorbed on mineral surfaces in salt solutions. Geochim Cosmochim Acta 70:2427–2453
Swainson IP, Schulson EM (2004) Invasion of ice through rigid anisotropic porous media. J Geophys Res 109:B12205
Tartatakovsky AM, Redden G, Lichtner PC, Scheibe TD, Meakin P (2008) Mixing-induced precipitation: Experimental study and multiscale numerical analysis. Water Resour Res 44:W06S04
Trainor TP, Chaka AM, Eng PJ, Newville M, Waychunas GA, Catalano JG, Brown GE Jr. (2004) Structure and reactivity of the hydrated hematite (0001) surface. Surf Sci 573:204–224
Verma A, Pruess K (1988) Thermohydrologic conditions and silica redistribution near high-level nuclear wastes emplaced in saturated geological formations. J. Geophys Res. 93:1159–1173
Warner NR, Christie CA, Jackson RB Vengosh A (2013) Impacts of shale gas wastewater disposal on water quality in western Pennsylvania. Environ Sci Technol 47:11849–11857.
Wang H-W, Anovitz LM, Burg A, Cole DR, Allard LF, Jackson AJ, Stack AG, Rother G (2013) Multi-scale characterization of pore evolution in a combustion metamorphic complex, Hatrurim basin, Israel: Combining (ultra) small-angle neutron scattering and image analysis. Geochim Cosmochim Acta 121: 339–362
Wasylenki LE, Dove PM, Wilson DS, De Yoreo JJ (2005) Nanoscale effects of strontium on calcite growth: An in situ AFM study in the absence of vital effects. Geochim Cosmochim Acta 69:3017–3027
Wesolowski DJ, Ziemniak SE, Anovitz, LM, Machesky ML, Bénézeth P, Palmer DA (2004) Solubility and surface adsorption characteristics of metal oxides. *In:* Palmer DA, Fernandez-Prini R., Harvey AH (eds) Aqueous Systems at Elevated Temperatures and Pressures Elsevier, London, p 493–595
White AF (2008) Quantitative approaches to characterizing natural chemical weathering rates. *In:* Kinetics of Water–Rock Interaction. Brantley, SL, Kubicki JD, White AF (eds) Springer: New York p 469-543
Wright KE, Hartmann T, Fujita Y (2011) Inducing mineral precipitation in groundwater by addition of phosphate. Geochem Trans 12:8
Yoon H, Valocchi AJ, Werth CJ, Dewers T (2012) Pore-scale simulation of mixing-induced calcium carbonate precipitation and dissolution in a microfluidic pore network. Water Resour Res 48:W02524
Zhang S, DePaolo DJ, Xu T, Zheng L (2013) Mineralization of carbon dioxide sequestered in volcanogenic sandstone reservoir rocks. Int J Greenh Gas Control 18:315–328
Zhang T, Gregory K, Hammack RW, Vidic RD (2014) Co-precipitation of radium with barium and strontium sulfate and its impact on the fate of radium during treatment of produced water from unconventional gas extraction. Environ Sci Technol 48:4596–4603
Zhao XS, Lu GQ, Whittaker AK, Millar GJ, Zhu HY (1997) Comprehensive study of surface chemistry of MCM-41 using ^{29}Si CP/MAS NMR, FTIR, Pyridine-TPD, and TGA. J Phys Chem B 101:6525–6531
Zucker, HA (2014) A Public Health Review of High Volume Hydraulic Fracturing for Shale Gas Development. New York State Department of Health.